RESEARCH ARTICLE

Novel electrospun poly(ε-caprolactone)/type I collagen nanofiber conduits for repair of peripheral nerve injury

Chun-Ming Yen[1, 2], Chiung-Chyi Shen[1, 3, 4], Yi-Chin Yang[1], Bai-Shuan Liu[5], Hsu-Tung Lee[1], Meei-Ling Sheu[6, 7, 8], Meng-Hsiun Tsai[9], Wen-Yu Cheng[1, 3, *]

1 Department of Neurosurgery, Neurological Institute, Taichung Veterans General Hospital, Taichung, Taiwan, China
2 Ph.D. Program in Translational Medicine, National Chung Hsing University, Taichung, Taiwan, China
3 Department of Physical Therapy, Hungkuang University, Taichung, Taiwan, China
4 Basic Medical Education Center, Central Taiwan University of Science and Technology, Taichung, Taiwan, China
5 Department of Medical Imaging and Radiological Sciences, Central Taiwan University of Science and Technology, Taichung, Taiwan, China
6 Institute of Biomedical Sciences, National Chung Hsing University, Taichung, Taiwan, China
7 Department of Medical Research, Taichung Veterans General Hospital, Taichung, Taiwan, China
8 Rong Hsing Research Center for Translational Medicine, National Chung Hsing University, Taichung, Taiwan, China
9 Department of Management Information System, National Chung Hsing University, Taichung, Taiwan, China

Funding: *This study was supported by grants from the Taichung Veterans General Hospital and Central Taiwan University of Science and Technology, No. TCVGH-CTUST1047701 (to CCS and BSL) and Taichung Veterans General Hospital, No. TCVGH-1034907C (to CCS), Taiwan, China.*

Abstract

Recent studies have shown the potential of artificially synthesized conduits in the repair of peripheral nerve injury. Natural biopolymers have received much attention because of their biocompatibility. To investigate the effects of novel electrospun absorbable poly(ε-caprolactone)/type I collagen nanofiber conduits (biopolymer nanofiber conduits) on the repair of peripheral nerve injury, we bridged 10-mm-long sciatic nerve defects with electrospun absorbable biopolymer nanofiber conduits, poly(ε-caprolactone) or silicone conduits in Sprague-Dawley rats. Rat neurologica1 function was weekly evaluated using sciatic function index within 8 weeks after repair. Eight weeks after repair, sciatic nerve myelin sheaths and axon morphology were observed by osmium tetroxide staining, hematoxylin-eosin staining, and transmission electron microscopy. S-100 (Schwann cell marker) and CD4 (inflammatory marker) immunoreactivities in sciatic nerve were detected by immunohistochemistry. In rats subjected to repair with electrospun absorbable biopolymer nanofiber conduits, no serious inflammatory reactions were observed in rat hind limbs, the morphology of myelin sheaths in the injured sciatic nerve was close to normal. CD4 immunoreactivity was obviously weaker in rats subjected to repair with electrospun absorbable biopolymer nanofiber conduits than in those subjected to repair with poly(ε-caprolactone) or silicone. Rats subjected to repair with electrospun absorbable biopolymer nanofiber conduits tended to have greater sciatic nerve function recovery than those receiving poly(ε-caprolactone) or silicone repair. These results suggest that electrospun absorbable poly(ε-caprolactone)/type I collagen nanofiber conduits have the potential of repairing sciatic nerve defects and exhibit good biocompatibility. All experimental procedures were approved by Institutional Animal Care and Use Committee of Taichung Veteran General Hospital, Taiwan, China (La-1031218) on October 2, 2014.

***Correspondence to:**
Wen-Yu Cheng, PhD,
wycheng07@yahoo.com.tw.

orcid:
0000-0003-4661-3809
(Wen-Yu Cheng)

doi: *10.4103/1673-5374.255997*

Received: *September 1, 2018*
Accepted: *March 8, 2019*

Key Words: *poly(ε-caprolactone); type I collagen; electrospinning; sciatic nerve; nerve conduit; immunohistostaining; walking track analysis; peripheral nerve injury*

Chinese Library Classification No. *R459.9; R361; R6*

Introduction

In the study of peripheral nerve injury or rupture, a physician usually starts with determining the degree of severity. Although nerves are able to regenerate, treatment can be provided through medicine and microsurgery and, in case of severe injuries, biomaterials. Due to differences in manufacturing processes and material quality, biomaterials have different effects on nerve regeneration (Stanec and Stanec, 1998; Gu et al., 2012). However, many existing types of nerve guidance conduits, such as hollow conductors (Yang et al., 2010), porous conduits (Hsieh et al., 2016), multi-channel conduits (Dinis et al., 2015), and stem cell and growth factor enhanced conduits (Shen et al., 2012; Zheng and Cui, 2012; Dinis et al., 2014), are united by a common objective of achieving the regeneration and functional recovery of nerves within a short amount of time.

Electorspun silk nanofiber technologies have been widely applied in recent years (Biazar et al., 2010). With regard to nerve guidance conduits, small diameter fibers enabled by nanotechnologies can increase the surface area of the used material (Panseri et al., 2008). Microporous structures and high-level porosity can improve cell adhesion and growth, stimulating the regeneration of nervous tissue and the differentiation of stem cells into nerve cells (Kim et al., 2016). One study tested the compressive strength of nerve guidance conduits coated with film-like chitosan structures fabricated using fiber electrospinning technology (Matsuda et al., 2007). In another study, Schwann cells were cultivated using

chitosan and poly(ε-caprolactone) (PCL) to determine the most appropriate chitosan/PCL ratio for cell proliferation and maintenance of cellular-type material (Prabhakaran et al., 2008). Furthermore, electric conduction using electrospun nanofibers combined with electrical stimulation was examined in terms of its effect on nerve cells (Lee et al., 2009).

Biomaterials can either directly or indirectly interact with the human body. Therefore, biological compatibility is the primary consideration when selecting biomaterials, followed by other individual requirements. PCL is a polymer that can improve the mechanical properties of biomaterials and the wall strength of nerve conduits (Moroder et al., 2011). Being absorbable and biodegradable, PCL does not require a follow-up surgery for its removal (Yu et al., 2015). To date, it has been used in bone nails, artificial skin materials, drug delivery systems, and intravascular stents (Dash and Konkimalla, 2012). Some studies have also reported the use of PCL for controlled drug release during osteoporosis treatment (Nair et al., 2016) and the use of PCL/chitosan blend scaffolds to heal burns, cuts, and diabetic wounds (Gholipour-Kanani et al., 2016). However, the hydrophobic nature of PCL reduces cell adhesion and proliferation. In this study, type I collagen was applied to enhance the hydrophilic property of the conduit surface and, thus, cell proliferation. Type I collagen is a natural macromolecule and the main interstitial protein in the human body (Weber et al., 1984). Its largest benefits include stimulation of wound healing and low immunoreaction (Weber et al., 1984). Duration of its absorption in human body can be controlled *via* different levels of concentration (Figueres Juher and Bases Perez, 2015). With regard to its current clinical applications, type I collagen is used in artificial skin fabrication, bone repair, and dental materials (Shevchenko et al., 2010). One study used type I collagen three-dimensional cell culture methods to differentiate platelet-derived growth factor and insulin from adipose-derived stem cells to treat arthritis and bone defects (Scioli et al., 2017). A literature pointed out that type I collagen fabricated to microstructure scaffold can efficiently promote the regeneration of spinal tissue (Altinova et al., 2014). In addition, some studies proposed the combined use of PCL and type I collagen in bone tissue scaffolds (Subramanian et al., 2015) and used tracheal scaffolds with cord blood stem cells to promote tracheal epithelial cell proliferation (Jang et al., 2014).

This study aimed to investigate the effects of electrospun biologically absorbable PCL/type I collagen nerve conduits on the functional recovery of injured sciatic nerves in rats.

Materials and Methods

Fabrication of electrospun nanofiber conduits

5% PCL (average Mn = 80 kDa; Sigma-Aldrich, Milwaukee, WI, USA) and 2% type I collagen (SunMax Biotechnology Co., Ltd., Tainan County, Taiwan, China) were dissolved in a 1,1,1,3,3,3-hexafluoroisopropanol (HFIP) solvent (Sigma-Aldrich, St. Louis, MO, USA) with the PCL to type I collagen ratios of 1:3, 2:2, and 3:1 and then fabricated into electrospun nanofiber conduits. The electrospinning device (Matsusada Precision Inc., Shiga, Japan) comprised an injector, a needle head, and an earth electrode. To fabricate electrospun nanofiber conduits, the uniformly mixed electrospinning solution was first transferred into a glass syringe with a 21-gauge stainless steel needle head, which was then set up on a syringe pump that was set to an easy flow rate of 2 mL/h and a voltage of 20 kV. From the needle head to the aluminum surface plate, the collection distance for the nanofibers was 20 cm. After the nanofibers were collected on a collection spool, a capillary tube was then used to spin them into a tubular shape to produce nanofiber conduits.

Field-emission scanning electron microscope imaging

To acquire highly magnified images, field-emission scanning electron microscope (FEI Quanta 400, Houston, Texas, USA) was adopted to investigate the microstructure of electrospun nanofiber conduits and nerve tissues. It was operated at a working distance of 3 mm, an acceleration voltage of 15 kV and a beam current of 1.6×10^{-6} A. The specimens were made conductive by depositing a 2 nm-thick layer of platinum using a Cressington Sputter Coater 108A operated at a working distance of 100 mm and a current of 20 mA. Photographs were captured for each section used in the final quantitative analysis (Shen et al., 2011). To measure the sizes of the nerve and nanofibers, 30–50% of the sciatic nerve section area was randomly selected from each nerve specimen using Image-Pro Plus (Media Cybernetics, Rockville, MD, USA).

Grouping for animal experimentation

Forty-eight adult male Sprague-Dawley rats (BioLASCO Taiwan Co., Ltd., China), weighing 250–300 g, were used in the experiments. These rats were randomly divided into four groups: Normal group (n = 12; animals without severed nerves and implants), silicone conduit group (n = 12; the cut nerve ends were bridged with a silicone conduit), PCL only group (n = 12; the cut nerve ends were bridged with PCL nerve conduits), and PCL + type I collagen group (n = 12; PCL + type I collagen by electrospinning method). Under anesthesia by administration of 4% isoflurane (Baxter, USA) in combination with oxygen using a small animal anesthesia machine (VMS, Matrix, NY, USA). The rats were shaved (from the left leg to the waist), disinfected, and scrubed using povidone iodine and 70% ethanol. Under sterile surgical conditions, an incision of about 2 cm in length was made on the left leg of a rat to expose the muscles underneath. Using a curved forcep, the muscles were separated and 10-mm-long sciatic nerve was removed. Next, the far-near suture pattern was applied and 10/0 sutures (Johnson-Johnson, New Brunswick, NJ, USA) were used to join the nerve conduit. Briefly, the break point of the sciatic nerve was ligated by 12-mm-long nerve conduits which were flanked by proximal and distal nerve stumps with a depth of 1 mm into the chamber, leaving a 10-mm gap between the stumps. Finally, the muscle and epidermis were sutured using 3/0 sutures (nylon, UNIK, Taiwan, China). Disinfection of the surgical site was

performed using iodine. The experimental animals were kept at room temperature and exposed to 12 hours of fully automatic fluorescent lighting (which was then switched off for 12 hours) to simulate natural sunshine in the animal laboratory. Feed and clean drinking water were provided daily, and the litter in the rat cage was replaced every 3 days to keep it clean. All experimental procedures were approved by Institutional Animal Care and Use Committee of Taichung Veteran General Hospital Taiwan, China (La-1031218) on October 2, 2014, Taiwan, China and were performed in accordance with the guidelines of the Animal Welfare Protection Act of the Department of Agriculture, Executive Yuan in Taiwan, China.

Walking track analysis

A walking track test was conducted weekly over 8 weeks (Yang et al., 2011). After staining the hind limbs of a rat using a red inkpad, the rat was then placed in a cylindrical paper box (the bottom of the inside of the box was covered by white paper), where the walking tracked test was then conducted. Statistical methods were applied to compare the hind limbs of the experimental rats to those of normal rats and, thus, to indirectly measure the extent of sciatic nerve recovery by calculating sciatic functional index (SFI). SFI was ranged from 0 to –100 and an SFI of –100 indicated total impairment of the sciatic nerve (Yang et al., 2011). The print length (PL, distance between the mid toe and heel), toe spread (TS, distance between the first and fifth toes), and inter-median toe spread (IT, distance between the second and fourth toes) were measured using the Image Pro® Plus software (Media Cybernetics, Rockville, MD, USA), and SFI values were calculated using the following formula (Bain et al., 1989).

Print length function (PLF) = (experimental PL – normal PL)/normal PL

Toe spread function (TSF) = (experimental TS – normal TS)/normal TS (1^{st} to 5^{th} toes)

Inter-median toe spread function (ITF) = (experimental IT – normal IT)/normal IT (2^{nd} to 4^{th} toes)

SFI = −38.3 (PLF) + 109.5 (TSF) + 13.3 (ITF) – 8.8

Histological assessment of hematoxylin-eosin staining

At 8 weeks after surgery, the animals in each group were sacrificed by introducing 100% carbon dioxide (CO_2) gas in the euthanasia chamber at a flow rate of 20–30% chamber volume per minute. The sciatic nerves on the rat right legs were removed to serve as the normal group, and on the rat left legs, the distal and proximal sciatic nerve sections in the middle segments of the electrospun nanofiber nerve conduits were removed. The nerves were fixed in 4% paraformaldehyde for 24 hours and subsequently washed using phosphate-buffered saline (PBS). The next step was hydration, which was performed by soaking the samples sequentially in 100% and 95% ethanol solutions. The samples were soaked in each solution for 1 minute and washed under running water for 5 minutes. The excess water was removed from the samples, which were then immersed in a hematoxylin (Merck KGaA, Darmstadt, Germany) solution for 3 minutes to perform a nuclear staining. Following this, the samples were washed under running water for 5 minutes and then immersed in an eosin (Sigma, Canada) solution for 1 minute to perform a nuclear staining. This was followed by dehydration, during which the samples were soaked sequentially in 95%, and 100% alcohol solutions. The hematoxylin-eosin (HE) stains were observed using an upright optical microscope (Nikon Eclipse E600 Nikon Corp., Tokyo, Japan), and their tissue morphology was photographed and recorded (Shen et al., 2011).

Immunohistochemical and osmium tetroxide staining

The sciatic nerve slices were serially blocked with for 10 minutes and 5% skim milk in PBS for 30 minutes. Subsequently, the nerves were incubated overnight at 4°C with rabbit anti-CD4 polyclonal antibody (conjugated with peridinin chlorophyll; 1:200, Bioss, MA, USA) and rabbit anti-S-100 polyclonal antibody (1:200, GeneTex, CA, USA). Schwann cells wrap the around axons in the peripheral nervous system (PNS) to form the sheath (Mata et al., 1990). S-100 represents Schwann cells, and therefore, a 3,3′-diaminobenzidine (DAB) brown color indicates Schwann cells. The helper (Bashur and Ramamurthi) cells appear on the proteins on the CD4 cell surface. Th cells and target cells stick to each other during antigen specializing process and there is more CD4 expression during an inflammatory response (Zenewicz et al., 2009). Subsequently, the sections were rinsed with PBS and incubated with a SuperPicture polymer detection kit (Invitrogen, Camarillo, CA, USA) for 10 minutes at room temperature and then were rinsed three times with PBS for 2 minutes. Finally, the sections were visualized by color development with DAB enhancer (3,3′-diaminobenzidine tetrahydrochloride, Fremont, CA, USA) and counterstained with hematoxylin. The immunostained sections were examined using the optical microscope (Nikon Eclipse E600 Nikon Corp., Tokyo, Japan). The other regenerated sciatic nerve tissue samples were fixed in 1% osmium tetroxide (Sigma-Aldrich, St. Louis, MO, USA), dehydrated in a graded ethanol series, embedded in Spurs' low viscosity resin, cut transversely into 4 μm thick sections, and stained with 0.1% toluidine blue after the operation.

Transmission electron microscopy analysis

The sciatic nerve tissue samples were fixed in 3% ice-glutaraldehyde for 12 hours, washed in buffer, post-fixed in 1% osmium tetroxide, washed in distilled water, dehydrated in increasing concentrations of ethanol, and embedded in resin for 24 hours. 75 nm ultra-thin cross-sections were cut and stained using methanolic uranyl acetate and lead citrate. Representative areas were chosen for ultra-thin sectioning and examined on transmission electron microscopy (JEOL JEM-1230 Tokyo, Japan) at 5000× magnification under operation at 80 kV.

Statistical analysis

The mean values and standard deviations relating to the

measurement data for each group are presented. One-way analysis of variance (ANOVA) was used to determine if there were differences between the groups. The differences between the experimental and control groups were then analyzed using the independent samples *t*-test, with $P < 0.05$ indicating a statistically significant difference in the results (Shen et al., 2011).

Results

Structural difference between two types of nanofibers

Figure 1A shows the nanofiber catheter. **Figures 1B** and **C** show the nanofibers in the PCL only and PCL + type I collagen groups, respectively, illustrating their linearity at 5000× magnification. **Figure 1D** shows nanofiber thickness. The average diameter of nanofiber in the PCL + type I collagen group was significantly shorter than that in the PCL only group ($P < 0.001$). Interestingly, the nanofiber diameters in the PCL + type I collagen group also had less variation than those in the PCL only group (coefficient of variation: 12.64% *vs*. 25.05%). Field-emission scanning electron microscope imaging results showed that the electrospun nanofibers were straight. Greater uniformity of the nanofibers' average diameter indicated stronger structure of the nanofiber conduit. A smaller difference in average value also allows for adsorptive capacity on the surface area to increase. A previous study compared the effect of a PCL nanofiber (diameter = 251 ± 32 nm) conduit and a microfiber (diameter = 981 ± 83 nm) conduit on the sciatic nerves of rats. Results showed that the compound muscle action potential (CMAP) of the nanofiber conduit was higher than that of the microfiber conduit, resulting in a higher number of axons and myelin sheaths (Jiang et al., 2014). The nanofiber diameter in the PCL + type I collagen group exhibited better uniformity which can provide a stronger nanofiber structure and thereby enhance the adsorptive properties of the large surface area (Beachley and Wen, 2009). Thus, our results showed that nanofibers in the PCL + type I collagen group possessed structural advantages as a bio-scaffold. In this study, electrospinning technology was successfully utilized to produce nanofiber-grade artificial nerve conduits from polymeric materials, with the average diameters of the nanofibers being maintained at 200–300 nm (**Figure 1**). Between the stack layers, web structures were formed, and conduits made from materials that possess these web structures will allow for nutrients inside and outside the conduit to be transferred across the conduit, which will facilitate the transfer of materials and prevent peripheral fibrous structures from entering the conduit and hindering nerve repair.

Biocompatibility of nanofiber conduits

Figure 2A displays the state of the nanofiber nerve conduits in the bodies of animals after being sacrificed at 8 weeks. The nanofiber conduits in the PCL + type I collagen group showed high biocompatibility with nervous tissues after 8 weeks. In the PCL + type I collagen group, there was no significant inflammatory response or swelling suppuration in peripheral tissue, and nanofiber nerve conduits did not collapse or disintegrate. After removal of the nerve tissue, nanofiber conduits in the PCL + type I collagen group were detached to expose internal nervous tissue, which well-regenerated and had similar diameter to that of normal nervous tissue. Nanofiber conduits in the PCL + type I collagen group did not dissolve within the animals at 8 weeks after surgery and can support the complete growth of the never tissue. At 8 weeks after surgery, the nanofiber conduits showed slight depression yet there was no evident inflammatory response. After the materials were removed, regenerated tissues connecting the two transactional sides of the nerve in the middle were also apparent. However, compared to the normal nerve tissues at the bottom, the regenerated tissues had finer diameters and, therefore, the effects of the regeneration been limited. At 8 weeks after surgery, the silicone conduit group showed obvious white regenerated nerve tissue in the silicone conduit. The conduit is full of light yellow tissue fluid with no inflammatory response. After removal of the conduit, nerve regeneration in the middle of the nerve was also visible. However, when compared with normal nerve tissue, the regenerated tissue in the middle of the silicone conduits was thinner in diameter. This may have been due to the lack of any absorbable neurotrophic factor in the conduit that caused the cessation of growth after 4–6 weeks.

Figure 2B compares the middles of regenerated nerves in each group using Image-Pro Plus computer-generated imagery software to measure their diameters. The middle diameter of the regenerated nerves in the PCL + type I collagen group was close to that in the normal group and their growing diameters were similar ($P > 0.05$), whereas the diameters of the middle regenerated nerves were similar between the silicone conduit and the PCL groups ($P < 0.05$). From these findings it was determined that after removal of mouse sciatic nerves, implantation of silicone conduit and/or PCL nanofiber conduit can facilitate nerve regeneration; however, the effects are limited as the estimated cessation of growth of the regenerated nerves occurred at 4–6 weeks. The truncated nerves in the PCL + type I collagen group were able to regenerate and the diameters of the regenerated nerves approached normal nerves.

Histological morphology and quantitative estimation for nerve fiber

Figure 3 shows the nerve specimens stained with osmic acid and hematoxylin-eosin from each group. At 100× magnification, osmic acid staining results showed that the normal and PCL + type I collagen groups had the largest nervous tissue areas, while the silicone conduit and PCL only groups had smaller areas. At 400× magnification, we observed that the normal group had clear black circles of myelin sheath of uniform size, while myelin sheaths in the PCL + type I collagen group were still growing with a few newborn blood vessels. In the silicone conduit group, there are more myelin sheaths in the middle, the area of regenerated nerve tissues was smaller, and the tissue morphology was more complete. In the PCL group, there was little sheath, but there were some newborn vessels with loose tissue structures and more

of nerve extension) was complete. In the PCL + type I collagen group, the undulating fibrous texture of the regenerating tissues promoted regeneration and repair (**Figure 3**).

S-100 and CD4 immunoreacitivities

Figure 4 shows the paraffin wax slices of immune tissues for each group chemically stained with S100 protein and CD4. The results showed that the normal group also had normal S-100 immunoreactivity. The PCL + type I collagen showed more S-100 staining than the other groups, which maybe because Schwann cells were repairing the lesions. The silicone conduit group was not stained by S-100 antibody and the tissues showed more vacuoles. The PCL only group also showed no S-100 staining. The normal and PCL + type I collagen groups were barely stained with CD4, whereas the silicone conduit and PCL only groups were stained with more CD4, indicating that these two groups had inflammatory responses.

Sciatic nerve function

Figure 5 shows SFI over an 8-week observation period, during which the functional recovery status of the rat hind limbs was recorded. When the sciatic nerves were broken, the nerve function was completely lost, and thus the average SFI value was –100. The SFI value in the PCL + type I collagen group after injury increased from –81.45 to –77.17 at week 4 and to –58.77 at week 8. The SFI value in the silicone conduit group after injury increased from –89.36 to –78.63 at week 6 and to –64.14 at week 8. The SFI value after injury was slightly lower in the silicone conduit group than in the PCL+ type I collagen group. In the PCL group, the SFI value increased from –91.12 to –75.01 at week 8. With regard to the functional assessment of the rat hind limbs, this study utilized a walking track test to analyze the differences between the groups. There was no significant difference in walking track test results between groups during the first week, but by the eighth week, the SFI value in the PCL + type I collagen group increased from –81.45 ± 8.73 to –58.77 ± 13.9. These findings suggest that PCL + type I collagen is the best solution among these three nerve conduits.

Transmission electron microscope analysis (**Figure 6**) of the regenerating sciatic nerve sections was performed after 8 weeks of treatment and showed that the myelin sheath of each axon was stained black after exposure to osmium tetroxide. In the normal group, the expression of many normal sciatic myelin sheaths was observed. A higher number of myelin sheaths were found in the PCL + type I collagen group than in the silicone conduit and PCL only groups. Higher levels of magnification allowed for observing the thickness of an entire myelin sheath. It was observed that the myelin sheaths of normal nerves had a dense, layered structure. In the PCL + type I collagen group, myelin sheaths were found to be thinner than those in the normal group, but also densely stacked. The thickness of myelin sheaths in the silicone conduit group was similar to that in the PCL + type I collagen group. However, there were a small number of broken axons in the silicone conduit group. Among all groups, the PCL group had the thinnest myelin sheaths, which were also observed to contain some broken axons.

Discussion

In this study, electrospinning technology was utilized to produce nanofiber-grade artificial nerve conduits from polymeric materials. The conduits were then inserted into the sciatic nerve amputation sites of rats, which were then observed for 8 weeks to assess the recovery of their neurological functions. Comparison of nanofiber diameters between the PCL only and PCL + type I collagen was first carried out. These results showed that the application of electrospinning nanotechnology had helped to improve nerve repair (Jiang et al., 2014). The use of spinal scaffolds made from collagen nanofibers (diameter = 208.2 ± 90.4 nm) promotes repair of acute spinal cord injury in rats. This showed that nanofibers can be used as scaffolds to repair damaged sections of the spinal cord (Liu et al., 2012). In this manner, a good tissue-engineered scaffold is created.

A previous study also found that this synthetic conduit could promote the repair of motor nerves and provide an ideal growth environment for nerve regeneration (Lee et al., 2012). These two materials were cultivated *in vitro* using 3D printing and chondrocytes, and may be used as scaffolds for the external ear (Walser et al., 2016). Another study indicated that the two materials could be combined and applied to tracheal reconstruction (Jang et al., 2014). Tissue engineering technology was utilized to create a good regenerative microenvironment in which truncated nerves can be repaired and regenerate, and the application of electrospinning technology strengthened the structure of a nerve conduit. This improved the conduit's mechanical properties and enabled control over the timing of the conduit decomposition in the body, with the purpose of improving tissue-engineered artificial nerve conduits and their functionality (Bashur and Ramamurthi, 2014). In still another study, nerve conduits made from certain materials were inserted into the body, and even though no signs of rejection were found over a period of 1 month or so, mild inflammation and fibroblastic proliferation were observed (Wang et al., 2015). An advantage of electrospinning is that it does not require any heating or chemical reaction during the synthesis of the nerve conduit. Therefore, for material reactions that exhibit unstable thermal or chemical properties and cannot be handled using other methods, electrospinning can be utilized to produce the required microfiber or nanofiber (Panseri et al., 2008). These results showed that the electrospun nanofiber conduits were able to induce the regeneration of truncated nerves, and that the web structures in these conduits were conducive to nerve cell proliferation. In future designs, such conduits can be designed to secrete various neurotrophic factors to further promote axon growth. The above results confirmed that the combined use of these two materials can be applied in tissue engineering (Lee et al., 2012).

In this study, osmic acid and HE staining were utilized to verify the state of axon regeneration and repair, and to observe the changes to cell types and tissues (Carriel et al.,

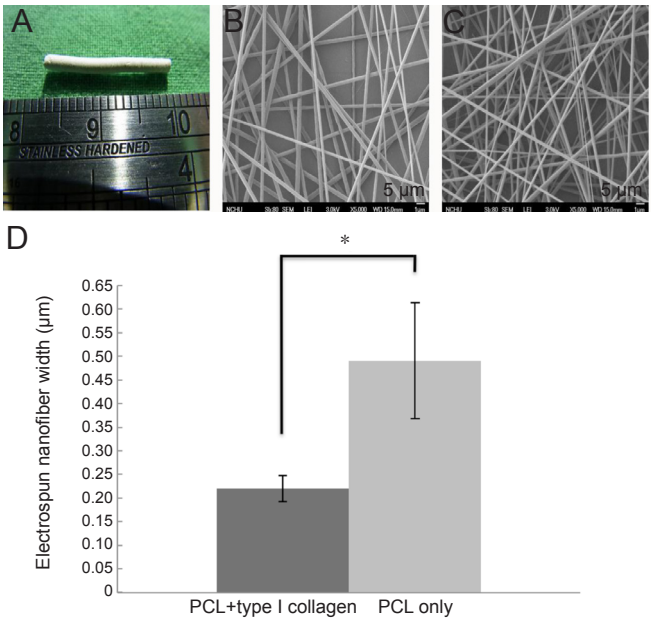

Figure 1 Structural identification of electrospun nanofibers.
(A–C) The gross appearance (A) and transmission electron microscopy morphology of the nanofiber in the PCL only group (B) and PCL + type I collagen group (C) (scale bars: 5 μm). (D) Histograms using Image-Pro Plus computer-generated imagery software to analyze fiber thickness (n = 12 for each group). Data are expressed as the mean ± SD. *P < 0.001 (independent samples t-test).

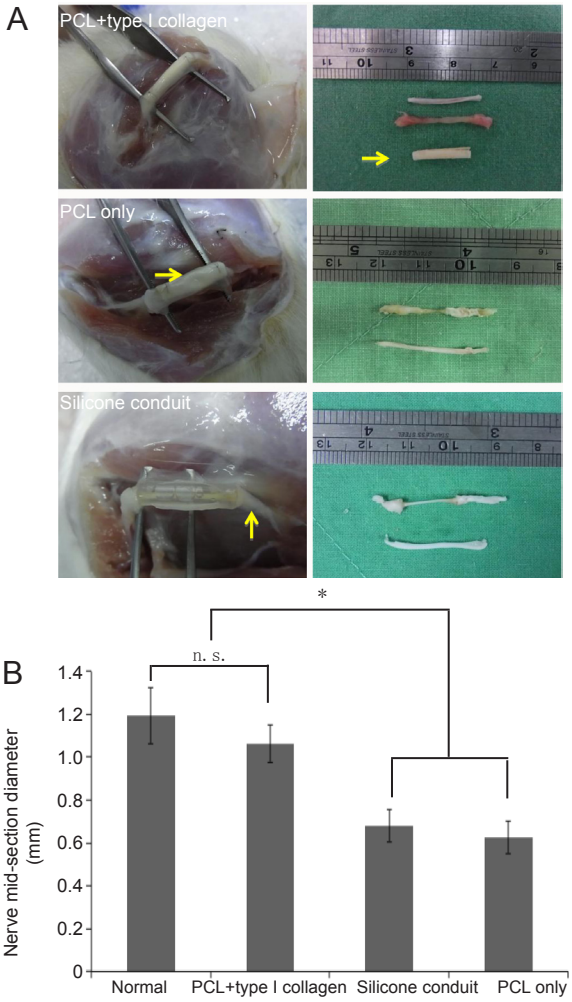

Figure 2 Macrographs of the nanofiber conduits at 8 weeks after implantation and regenerative nerve diameter.
(A) The nanofiber conduits in the bodies of animals after being sacrificed at 8 weeks after surgery. The yellow arrows indicate nanofiber conduit at 8 weeks *in vivo*. (B) Nerve mid-section diameters in each group measured by Image-Pro Plus computer-generated imagery software. Data are expressed as the mean ± SD (n = 12 for each group). n.s. indicates non-significant. *P < 0.05 (one-way analysis of variance).

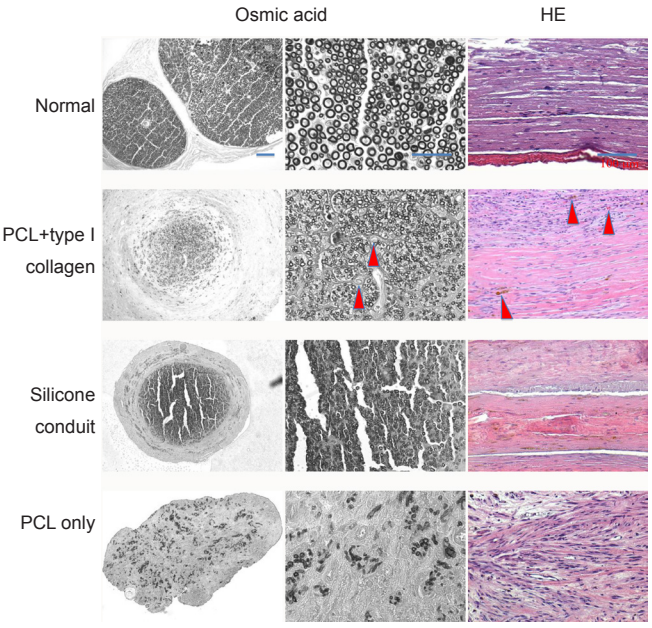

Figure 3 Histological morphology of the sciatic nerve stained in osmic acid and HE at 8 weeks after surgery.
All sections from each group were examined using the optical microscope. Upon osmic acid staining, the myelin sheaths of regenerated nerve were visualized (left and middle panels). In the right panels, HE images illustrate the corresponding cell types existing in each type of nerve conduit. The red arrowheads in middle panel indicate extended blood vessels while red arrowheads in the right panel indicate red blood cells. HE: Hematoxylin-eosin.

distributed black circles of sheath. The tissue morphologies were visualized on 200× magnified images from hematoxylin-eosin staining. The normal group displayed neatly arranged sciatic nerve fiber tissues. The PCL + type I collagen group had a lot of red blood cells in the tissue, but the nerve fibers were not arranged neatly, indicating that the recovery was still in progress. The silicone conduit group had slightly arranged nerve fibers above and below. The PCL only group had disordered nerve tissue with large spaces in between, indicating poor recovery. In the PCL + type I collagen group, newly formed blood vessels and nerve tissues were similar to those in the normal group, and their myelin sheaths were still growing (**Figure 3**). When magnified, the transverse sections of the nerve tissues stained with hematoxylin-eosin from the normal group showed that the undulating fibrous texture of its sciatic nerve fibers (which function to increase the range

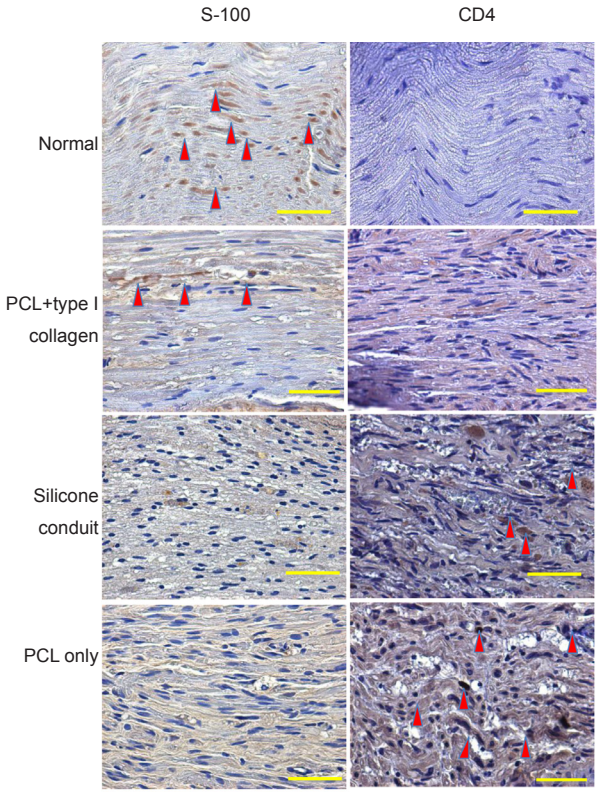

Figure 4 Immunohistochemical staining for S-100 and CD4 in the sciatic nerve repaired by nerve conduits in each group at 8 weeks after surgery.

All sections from each group were examined using the optical microscope. The existence of Schwann cells was validated using primary antibody against S-100 protein (marker for Schwann cells; arrowheads in left panels). The accumulations of $CD4^+$ cells (marker for T cells) can be also visualized to represent the severity of T-cell response (arrows in right panels). S-100-immunoreactive cells exhibit the brown 3,3′-diaminobenzidine color (*i.e.*, Schwann cells). Scale bars: 50 μm.

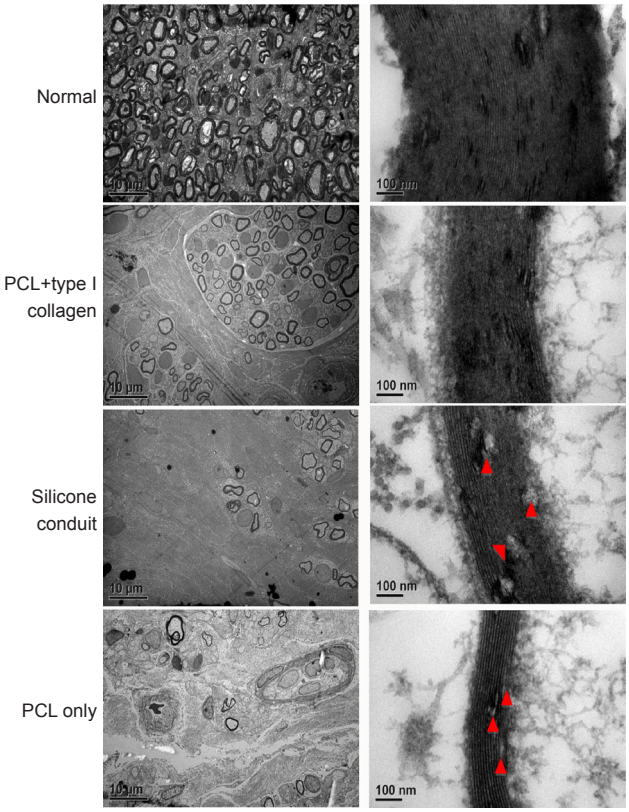

Figure 6 Ultrastructure of regenerated tissue in each group at 8 weeks after surgery.

Representative transmission electron microscope images showing vertical views of nerve fiber structure under two different magnifications. The distribution of sheathed nerve fibers can be visualized under 5000× original magnification (left panels). When increasing the magnification to 20,000×, clear views of layered myelin sheaths of each nerve fiber can be watched (right panels). The red arrowheads indicate axons with broke myelin sheaths.

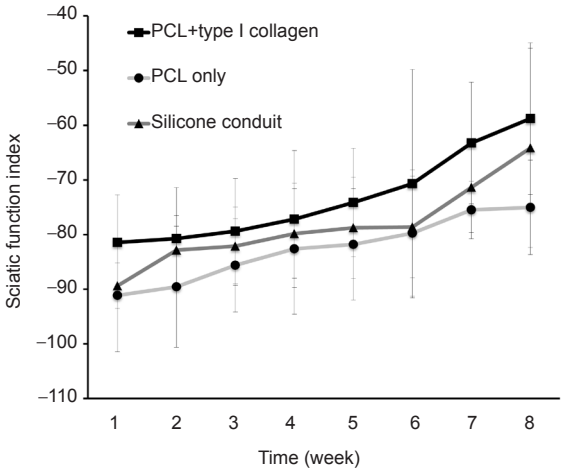

Figure 5 Sciatic nerve function of rats over 8 weeks after nanofiber nerve conduit repair.

Functional recovery status of the rat hind limbs was assessed using sciatic function index. Representative line graph showing the average sciatic function index recorded from every week over 8 weeks of study period. When the sciatic nerves were broken, the nerve function was completely lost; thus, the average sciatic function index was –100.

2014). The above experimental results proved that the nanofiber nerve conduits in the PCL + type I collagen group had retained the required biocompatibility and good mechanical properties that are needed to promote peripheral nerve regeneration. Past studies have pointed out that good biomedical materials can reduce the duration of inflammation, exhibit low immunity, and be broken down and absorbed by the body for use in wound healing (Gonzalez-Perez et al., 2017). This study found that the Schwann cells in the normal and PCL + type I collagen groups enveloped the axons in the peripheral nervous system to form myelin sheaths. $CD4^+$ T helper cells were also observed. During antigen-specific responses, these T helper cells can bind themselves closely to target cells. The experimental results revealed that more CD4+ cells were stained in the silicone and PCL only groups, indicating that these two materials induced a stronger inflammatory response in the tissues.

SFI results proved the ability of nanofiber conduits made of PCL and type I collagen can enhance nerve regeneration and recover neural functionality to a certain degree. Moreover, osmic acid staining and immunohistostaining were conducted after removing the nanofiber conduits from the

Table 1 Quantitative estimation of the regenerated nerve tissue of rats in each group at 8 weeks after implantation

Morphometric parameters	Normal group	PCL+type I collagen group	Silicone conduit group	PCL only group
Myelin sheath thickness (μm)	0.21±0.03	0.12±0.02	0.11±0.01	0.1±0.01
Nerve fiber number[a]	1891.5±119.0	1572.8±202.0	1084.3±127.0	793.1±205.0
Nerve fiber diameter (μm)	0.60±0.11	0.27±0.08	0.26±0.08	0.22±0.06
Blood vessel number[a]	2.30±0.98	1.50±1.08	0.50±0.52	0.30±0.48
Medial nerve area (μm^2)	14200.68±89.90	12483.14±4.43	6348.58±770.67	2894.51±111.12

[a] The number of nerve fibers or blood vessels was counted on vertical view of images.

sciatic nerves to evaluate myelination and inflammation in the rats. The results indicated no severe inflammation in the hind limbs of rats in which nerve conduits made of PCL and type I collagen were implanted and that Schwann cells were present in the injured area to promote regeneration. Within 8 weeks, the applied conduits promoted nerve regeneration and had the tendency in the recovery of hind limb function. The integration of nerve growth factors or neural stem cells can be considered in future research. The proposed method maybe clinically applied in patients with nerve injuries. Results from this study showed that rat hindlimb toes were gradually spreading, indicating that their hindlimb functions had recovered significantly. To date, few studies on nanofiber nerve conduits have utilized transmission electron microscope to analyze recoveries from sciatic nerve injuries. The use of transmission electron microscope in this study made it possible to clearly observe that the myelin sheath of each axon was stained black after exposure to osmium tetroxide. The growth rate of axons determines the state of peripheral nerve regeneration. In the PCL + type I collagen group, a natural microenvironment for neurons and simulated nerve regeneration was created and axon growth was accelerated. The experimental data showed that the nanofiber conduits provided a structured scaffold and a source of nutrition. The tissue-engineered conduits were capable of innervating, such that tissue defect sites were able to gain functional muscle tissues. The nanofiber nerve conduits from the PCL + type I group may assist the repair of sciatic nerves. In the future, they can also be used with a variety of stem cells and neurotrophic factors to restore structures and functions.

Conclusions

The experimental results, mid-section nerve tissue regeneration test, and functional recovery assessment for animals were utilized in this study to prove that the biologically absorbable and electrospun nanofiber nerve conduits were capable of stimulating and inducing the functional recovery of injured sciatic nerves in rats. However, the most appropriate method for promoting the effective recovery of neural functions is still the implementation of postoperative electrostimulation and physical therapy (Doyle and Roberts, 2006; English et al., 2007). So far, a nanofiber conduit is still not used as an alternative implant for supporting neuron regeneration in surgical treatment. Despite the results of the present study do not show significant improvement of functional and behavioral recovery in nanofiber conduit-implanted rats, this biomaterial is able to support the integrity and regeneration of neurons without inducing inflammation. Therefore, nanofiber conduits may have potential to be used as an accessory tool in the treatment of central nervous system traumatic injury.

Author contributions: *Design, implementation, and supervision of experiments, manuscript preparation: CMY, WYC; animal experiments and fabrication of electrospun nanofiber conduits: CCS, YCY; walking track analysis and histological assessment: BSL, HTL; manuscript preparation and statistical analysis: MLS, MHT; approval of final manuscript for publication: all authors.*
Conflicts of interest: *The authors declare no competing financial interest.*
Financial support: *This study was supported by grants from the Taichung Veterans General Hospital and Central Taiwan University of Science and Technology, No. TCVGH-CTUST1047701 (to CCS and BSL) and Taichung Veterans General Hospital, No. TCVGH-1034907C (to CCS), Taiwan, China.*
Institutional review board statement: *All experimental procedures were approved by Institutional Animal Care and Use Committee of Taichung Veteran General Hospital, Taichung, Taiwan, China (La-1031218) on October 2, 2014.*
Copyright license agreement: *The Copyright License Agreement has been signed by all authors before publication.*
Data sharing statement: *Datasets analyzed during the current study are available from the corresponding author on reasonable request.*
Plagiarism check: *Checked twice by iThenticate.*
Peer review: *Externally peer reviewed.*

Open peer reviewer: *Aldo Calliari, Veterinary School - UdelaR, Uruguay.*
Additional file: *Open peer review report 1.*

References

Altinova H, Mollers S, Fuhrmann T, Deumens R, Bozkurt A, Heschel I, Damink LH, Schugner F, Weis J, Brook GA (2014) Functional improvement following implantation of a microstructured, type-I collagen scaffold into experimental injuries of the adult rat spinal cord. Brain Res 1585:37-50.

Bain JR, Mackinnon SE, Hunter DA (1989) Functional evaluation of complete sciatic, peroneal, and posterior tibial nerve lesions in the rat. Plast Reconstr Surg 83:129-138.

Bashur CA, Ramamurthi A (2014) Composition of intraperitoneally implanted electrospun conduits modulates cellular elastic matrix generation. Acta Biomater 10:163-172.

Beachley V, Wen X (2009) Effect of electrospinning parameters on the nanofiber diameter and length. Mater Sci Eng C Mater Biol Appl 29:663-668.

Biazar E, Khorasani MT, Montazeri N, Pourshamsian K, Daliri M, Rezaei M, Jabarvand M, Khoshzaban A, Heidari S, Jafarpour M, Roviemiab Z (2010) Types of neural guides and using nanotechnology for peripheral nerve reconstruction. Int J Nanomedicine 5:839-852.

Carriel V, Garzon I, Alaminos M, Cornelissen M (2014) Histological assessment in peripheral nerve tissue engineering. Neural Regen Res 9:1657-1660.

Dash TK, Konkimalla VB (2012) Poly-small je, Ukrainian-caprolactone based formulations for drug delivery and tissue engineering: A review. J Control Release 158:15-33.

Dinis TM, Elia R, Vidal G, Dermigny Q, Denoeud C, Kaplan DL, Egles C, Marin F (2015) 3D multi-channel bi-functionalized silk electrospun conduits for peripheral nerve regeneration. J Mech Behav Biomed Mater 41:43-55.

Dinis TM, Vidal G, Jose RR, Vigneron P, Bresson D, Fitzpatrick V, Marin F, Kaplan DL, Egles C (2014) Complementary effects of two growth factors in multifunctionalized silk nanofibers for nerve reconstruction. PLoS One 9:e109770.

Doyle LM, Roberts BL (2006) Exercise enhances axonal growth and functional recovery in the regenerating spinal cord. Neuroscience 141:321-327.

English AW, Schwartz G, Meador W, Sabatier MJ, Mulligan A (2007) Electrical stimulation promotes peripheral axon regeneration by enhanced neuronal neurotrophin signaling. Dev Neurobiol 67:158-172.

Figueres Juher T, Bases Perez E (2015) An overview of the beneficial effects of hydrolysed collagen intake on joint and bone health and on skin ageing. Nutr Hosp 32 Suppl 1:62-66.

Gholipour-Kanani A, Bahrami SH, Rabbani S (2016) Effect of novel blend nanofibrous scaffolds on diabetic wounds healing. IET Nanobiotechnol 10:1-7.

Gonzalez-Perez F, Cobianchi S, Heimann C, Phillips JB, Udina E, Navarro X (2017) Stabilization, rolling, and addition of other extracellular matrix proteins to collagen hydrogels improve regeneration in chitosan guides for long peripheral nerve gaps in rats. Neurosurgery 80:465-474.

Gu J, Hu W, Deng A, Zhao Q, Lu S, Gu X (2012) Surgical repair of a 30 mm long human median nerve defect in the distal forearm by implantation of a chitosan-PGA nerve guidance conduit. J Tissue Eng Regen Med 6:163-168.

Hsieh SC, Chang CJ, Cheng WT, Tseng TC, Hsu SH (2016) Effect of an epineurial-like biohybrid nerve conduit on nerve regeneration. Cell Transplant 25:559-574.

Jang YS, Jang CH, Cho YB, Kim M, Kim GH (2014) Tracheal regeneration using polycaprolactone/collagen-nanofiber coated with umbilical cord serum after partial resection. Int J Pediatr Otorhinolaryngol 78:2237-2243.

Jiang X, Mi R, Hoke A, Chew SY (2014) Nanofibrous nerve conduit-enhanced peripheral nerve regeneration. J Tissue Eng Regen Med 8:377-385.

Kim JI, Hwang TI, Aguilar LE, Park CH, Kim CS (2016) A controlled design of aligned and random nanofibers for 3D bi-functionalized nerve conduits fabricated via a novel electrospinning set-up. Sci Rep 6:23761.

Lee BK, Ju YM, Cho JG, Jackson JD, Lee SJ, Atala A, Yoo JJ (2012) End-to-side neurorrhaphy using an electrospun PCL/collagen nerve conduit for complex peripheral motor nerve regeneration. Biomaterials 33:9027-9036.

Lee JY, Bashur CA, Goldstein AS, Schmidt CE (2009) Polypyrrole-coated electrospun PLGA nanofibers for neural tissue applications. Biomaterials 30:4325-4335.

Liu T, Houle JD, Xu J, Chan BP, Chew SY (2012) Nanofibrous collagen nerve conduits for spinal cord repair. Tissue Eng Part A 18:1057-1066.

Mata M, Alessi D, Fink DJ (1990) S100 is preferentially distributed in myelin-forming Schwann cells. J Neurocytol 19:432-442.

Matsuda A, Kagata G, Kino R, Tanaka J (2007) Preparation of chitosan nanofiber tube by electrospinning. J Nanosci Nanotechnol 7:852-855.

Moroder P, Runge MB, Wang H, Ruesink T, Lu L, Spinner RJ, Windebank AJ, Yaszemski MJ (2011) Material properties and electrical stimulation regimens of polycaprolactone fumarate-polypyrrole scaffolds as potential conductive nerve conduits. Acta Biomater 7:944-953.

Nair BP, Sindhu M, Nair PD (2016) Polycaprolactone-laponite composite scaffold releasing strontium ranelate for bone tissue engineering applications. Colloids Surf B Biointerfaces 143:423-430.

Panseri S, Cunha C, Lowery J, Del Carro U, Taraballi F, Amadio S, Vescovi A, Gelain F (2008) Electrospun micro- and nanofiber tubes for functional nervous regeneration in sciatic nerve transections. BMC Biotechnol 8:39.

Prabhakaran MP, Venugopal JR, Chyan TT, Hai LB, Chan CK, Lim AY, Ramakrishna S (2008) Electrospun biocomposite nanofibrous scaffolds for neural tissue engineering. Tissue Eng Part A 14:1787-1797.

Scioli MG, Bielli A, Gentile P, Cervelli V, Orlandi A (2017) Combined treatment with platelet-rich plasma and insulin favours chondrogenic and osteogenic differentiation of human adipose-derived stem cells in three-dimensional collagen scaffolds. J Tissue Eng Regen Med 11:2398-2410.

Shen CC, Yang YC, Liu BS (2011) Large-area irradiated low-level laser effect in a biodegradable nerve guide conduit on neural regeneration of peripheral nerve injury in rats. Injury 42:803-813.

Shen CC, Yang YC, Liu BS (2012) Peripheral nerve repair of transplanted undifferentiated adipose tissue-derived stem cells in a biodegradable reinforced nerve conduit. J Biomed Mater Res A 100:48-63.

Shevchenko RV, James SL, James SE (2010) A review of tissue-engineered skin bioconstructs available for skin reconstruction. J R Soc Interface 7:229-258.

Stanec S, Stanec Z (1998) Ulnar nerve reconstruction with an expanded polytetrafluoroethylene conduit. Br J Plast Surg 51:637-639.

Subramanian G, Bialorucki C, Yildirim-Ayan E (2015) Nanofibrous yet injectable polycaprolactone-collagen bone tissue scaffold with osteoprogenitor cells and controlled release of bone morphogenetic protein-2. Mater Sci Eng C Mater Biol Appl 51:16-27.

Walser J, Stok KS, Caversaccio MD, Ferguson SJ (2016) Direct electrospinning of 3D auricle-shaped scaffolds for tissue engineering applications. Biofabrication 8:025007.

Wang YL, Gu XM, Kong Y, Feng QL, Yang YM (2015) Electrospun and woven silk fibroin/poly(lactic-co-glycolic acid) nerve guidance conduits for repairing peripheral nerve injury. Neural Regen Res 10:1635-1642.

Weber L, Kirsch E, Muller P, Krieg T (1984) Collagen type distribution and macromolecular organization of connective tissue in different layers of human skin. J Invest Dermatol 82:156-160.

Yang YC, Shen CC, Cheng HC, Liu BS (2011) Sciatic nerve repair by reinforced nerve conduits made of gelatin-tricalcium phosphate composites. J Biomed Mater Res A 96:288-300.

Yang YC, Shen CC, Huang TB, Chang SH, Cheng HC, Liu BS (2010) Characteristics and biocompatibility of a biodegradable genipin-cross-linked gelatin/beta-tricalcium phosphate reinforced nerve guide conduit. J Biomed Mater Res B Appl Biomater 95:207-217.

Yu YH, Fan CL, Hsu YH, Chou YC, Ueng SWN, Liu SJ (2015) A novel biodegradable polycaprolactone fixator for osteosynthesis surgery of rib fracture: in vitro and in vivo study. Materials (Basel) 8:7714-7722.

Zenewicz LA, Antov A, Flavell RA (2009) CD4 T-cell differentiation and inflammatory bowel disease. Trends Mol Med 15:199-207.

Zheng L, Cui HF (2012) Enhancement of nerve regeneration along a chitosan conduit combined with bone marrow mesenchymal stem cells. J Mater Sci Mater Med 23:2291-2302.

P-Reviewer: Calliari A; C-Editor: Zhao M; S-Editor: Li CH; L-Editor: Song LP; T-Editor: Jia Y